

Two-Term Asymptotic Approximation of a Cardiac Restitution Curve*

John W. Cain[†]
David G. Schaeffer[‡]

Abstract. If spatial extent is neglected, ionic models of cardiac cells consist of systems of ordinary differential equations (ODEs) which have the property of excitability, i.e., a brief stimulus produces a prolonged evolution (called an action potential in the cardiac context) before the eventual return to equilibrium. Under repeated stimulation, or pacing, cardiac tissue exhibits electrical restitution: the steady-state action potential duration (APD) at a given pacing period B shortens as B is decreased. Independent of ionic models, restitution is often modeled phenomenologically by a one-dimensional mapping of the form $\text{APD}_{\text{next}} = f(B - \text{APD}_{\text{previous}})$. Under some circumstances, a restitution function f can be derived as an asymptotic approximation to the behavior of an ionic model.

In this paper, extending previous work, we derive the next term in such an asymptotic approximation for a particular ionic model consisting of two ODEs. The two-term approximation exhibits excellent quantitative agreement with the actual restitution curve, whereas the leading-order approximation significantly underestimates actual APD values.

Key words. asymptotic expansion, cardiac restitution curve, mapping model, ionic model, alternans

AMS subject classifications. 92C50, 34E05, 34C60

DOI. 10.1137/050632907

I. Introduction. Cardiac tissue is an example of an excitable medium. Applying a sufficiently strong stimulus to a cardiac cell leads to a prolonged elevation of transmembrane voltage v known as an *action potential*. When spatial extent is negligible, the cardiac action potential can be modeled by systems of nonlinear ODEs [1, 19]. Such models are referred to as *ionic models* because they describe the transport of various ions across the cell membrane.

Modeling the flow of transmembrane ionic currents represents one of the biggest challenges in cardiac electrophysiology [16], and many authors have proposed ionic models [1, 5, 8, 12, 18, 19, 20, 21, 23, 25]. An excellent database of the most well known models appears at <http://www.cellml.org/examples/repository/index.html>, and a listing of selected ionic models appears in Table 1. We remark that ionic models come in a variety of flavors—some are specific to certain types of cardiac cells, some are specific to certain animals, and some are especially concerned with accurate handling

*Received by the editors June 1, 2005; accepted for publication (in revised form) December 12, 2005; published electronically August 1, 2006. This work was supported by the National Science Foundation under grants DMS-9983320 and DMS-0244492 and by the National Institutes of Health under grant 1R01-HL-72831.

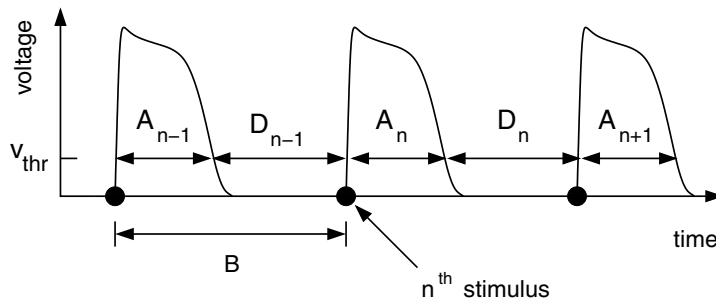
<http://www.siam.org/journals/sirev/48-3/63290.html>

[†]Department of Mathematics, Duke University, Durham, NC 27708 (jwcain@vcu.edu).

[‡]Department of Mathematics and Center for Nonlinear and Complex Systems, Duke University, Durham, NC 27708 (dgs@math.duke.edu).

Table I Selected ionic models of the cardiac action potential.

Model	Year	Tissue type	Remarks
Noble	1962	Purkinje fiber	one of the first adaptations of the Hodgkin–Huxley model to cardiac tissue
Beeler–Reuter	1977	mammalian, ventricular	uses four ionic currents; among the first models of the ventricular action potential
Luo–Rudy	1994	guinea pig, ventricular	a pioneering study for the handling of calcium dynamics
Jafri–Rice–Winslow	1998	ventricular	incorporates more sophisticated calcium handling
Courtemanche et al.	1998	human, atrial	uses human experimental data to formulate the various ionic currents

**Fig. 1** Schematic action potentials.

of particular ions. For example, the Luo–Rudy dynamic model [19], developed in part from guinea pig ventricular data, was among the first models to treat calcium cycling between the intracellular space and the sarcoplasmic reticulum. Although ionic models have been developed for many types of cells, most models are similar in spirit to the well-known Hodgkin–Huxley model [10] of the nerve action potential.

Not surprisingly, ionic models that are “more physiological” tend to be more complex mathematically. Among the simplest ionic models is the Fenton–Karma model [8], which expresses the total transmembrane current as the sum of three ionic currents. The Fenton–Karma model mimics the dynamics of the Beeler–Reuter model [1], which uses four ionic currents and a total of eight state variables. The Luo–Rudy dynamic model [19] incorporates a total of fourteen ionic currents and pumps.

Because cardiac arrhythmias are often characterized by *temporal* phenomena (i.e., timing of excitation and recovery), one frequently considers the *duration* of action potentials, not the complete voltage trace. To establish notation, refer to Figure 1, which shows a voltage trace of several consecutive action potentials in a repeatedly stimulated, or *paced*, cardiac cell. By specifying a threshold voltage v_{thr} , one may define the *action potential duration* (APD) as the amount of time in which $v > v_{\text{thr}}$ during an excitation. The subsequent recovery time during which $v < v_{\text{thr}}$ is called the *diastolic interval* (DI). We will denote the APD following the n th stimulus by A_n and the subsequent DI by D_n (see Figure 1).

Based on their experimental work, Nolasco and Dahlen [22] proposed a phenomenological mapping model to describe the dynamics of a paced cell, i.e.,

$$(1) \quad A_{n+1} = f(D_n) = f(B - A_n),$$

where B denotes the pacing period. The graph of f , known as the *restitution curve* (RC), is qualitatively similar to the graph of

$$(2) \quad f(\text{DI}) = \text{APD}_{\max} - Ce^{-\text{DI}/\tau}, \quad \text{APD}_{\max}, C, \tau > 0.$$

Although the approximation (1) is unrealistically simple,¹ it nonetheless adequately models some important phenomena. In particular, (i) for slow pacing rates (large B), the cell exhibits a phase-locked 1:1 response in which every stimulus yields an identical action potential, that is, the mapping (1) has a unique, stable fixed point [26]; and (ii) as shown by Guevara et al. [9], *alternans*, an abnormal beat-to-beat alternation of APD values, can result from a period-doubling bifurcation of (1) as the parameter B is gradually decreased. The fact that alternans has been linked to the onset of ventricular fibrillation and sudden cardiac death [15, 24, 27] alludes to the potential clinical use of RCs. Namely, it is believed that slopes of RCs can be used to predict the transition from normal 1:1 rhythms to alternans [9, 13].

In this paper, rather than introducing an ad hoc RC based on fitting experimental data, we derive an approximation of an RC as the asymptotic limit of a particular idealized ionic model. The first term of this asymptotic expansion, which was derived in [20], can significantly underestimate the actual APD values from the ionic model. Here, we derive the second term of the expansion, and this approximation exhibits excellent quantitative agreement with the actual RC.

Independent of the cardiac application, the derivation has pedagogical interest because it involves a common phenomenon in asymptotics, i.e., “falling off a nullcline” that turns back on itself. Other examples of this phenomenon arise in the context of the van der Pol relaxation oscillator [3, 17] and the singular Fitzhugh–Nagumo equation [6]. In a different context, a similar phenomenon is analyzed in [2]. This situation leads to a singular expansion with fractional powers and logarithms of the small parameter [17]. We believe that our straightforward exposition enhances the pedagogical potential of this problem.

1.1. A Two-Current Ionic Model. We recall the two-current model [14, 20] consisting of two ODEs. The notation is summarized in Table 2.

The *voltage equation* has the form

$$(3) \quad \frac{dv}{dt} = J_{\text{in}}(v, h) + J_{\text{out}}(v) + J_{\text{stim}}(t),$$

where J_{in} , J_{out} , and J_{stim} denote inward, outward, and stimulus currents, respectively. The stimulus current is discussed below. The inward and outward currents are given by

$$(4) \quad J_{\text{in}}(v, h) = \frac{h}{\tau_{\text{in}}} v^2 (1 - v),$$

$$(5) \quad J_{\text{out}}(v) = -\frac{v}{\tau_{\text{out}}},$$

¹For example, the model (1) does not exhibit any rate dependence or memory [4, 13]. See [25] for a two-dimensional mapping model with memory that may be derived as the asymptotic limit of an idealized ionic model.

Table 2 Summary of notation associated with the two-current model.

Symbol	Meaning	Units	Typical value(s)
v	scaled voltage	dimensionless	[0,1]
h	gate variable	dimensionless	[0,1]
τ_{in}	time constant	milliseconds	0.1
τ_{out}	time constant	milliseconds	2.4
τ_{open}	time constant	milliseconds	130
τ_{close}	time constant	milliseconds	150
v_{crit}	critical voltage	dimensionless	0.13
h_{min}	$4\tau_{\text{in}}/\tau_{\text{out}}$	dimensionless	0.17

where τ_{in} and τ_{out} are time constants. The *gate variable* h , which ranges from 0 to 1, represents a nondimensionalized conductance and regulates the flow of inward current. We assume that h obeys the *gate equation*

$$(6) \quad \frac{dh}{dt} = \begin{cases} \frac{1-h}{\tau_{\text{open}}}, & v \leq v_{\text{crit}}, \\ \frac{-h}{\tau_{\text{close}}}, & v > v_{\text{crit}}, \end{cases}$$

where τ_{open} and τ_{close} are time constants and v_{crit} represents a critical voltage. For voltages $v < v_{\text{crit}}$, the gate “opens,” allowing the flow of inward current. For voltages $v > v_{\text{crit}}$, the gate “closes” and shuts off the flow of inward current. For convenience, we set $v_{\text{thr}} = v_{\text{crit}}$ so that the APD is the amount of time in which $v > v_{\text{crit}}$ during an action potential. We shall not specify a functional form for the stimulus current J_{stim} , requiring only that it satisfy two conditions:

- $J_{\text{stim}}(t)$ is periodic with period B , and
- each stimulus consists of a brief (duration $\ll \tau_{\text{in}}$) pulse of current of sufficient strength to elicit an action potential.

We shall assume that the time constants satisfy

$$(7) \quad \tau_{\text{in}} \ll \tau_{\text{out}} \ll \tau_{\text{open}}, \tau_{\text{close}}.$$

Thus, in the absence of a stimulus current, the voltage changes more rapidly than the gate variable unless (v, h) is close to a nullcline of (3). Note that (3) has two nullclines: the trivial nullcline $v = 0$ and the nullcline given by

$$(8) \quad h = \frac{\tau_{\text{in}}}{\tau_{\text{out}}v(1-v)} \quad (0 < v < 1).$$

Equivalently, we may solve (8) for v :

$$(9) \quad v = v_{\pm}(h) = \frac{1}{2} \pm \frac{1}{2} \sqrt{1 - \frac{h_{\text{min}}}{h}},$$

where

$$(10) \quad h_{\text{min}} = \frac{4\tau_{\text{in}}}{\tau_{\text{out}}}$$

denotes the minimum value of h on the nullcline. We refer to $v_{+}(h)$ as the *excited branch* of the nullcline.

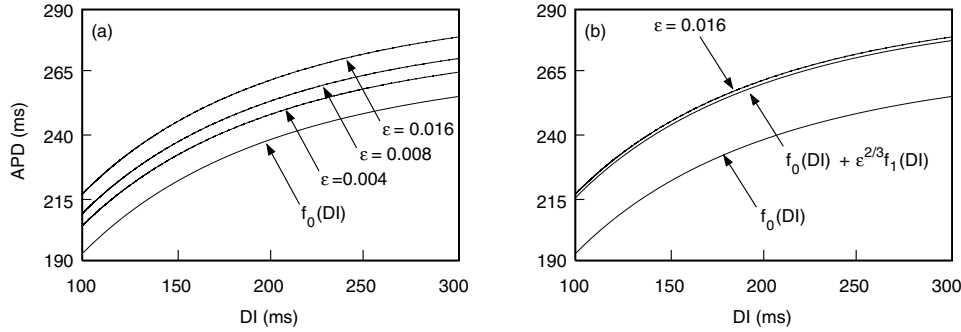


Fig. 2 (a) Comparison of $f_0(\text{DI})$ with actual RCs for several choices of ϵ . (b) Comparison of the leading-order and two-term approximations with the actual RC for a particular value of ϵ . In both panels, the uppermost curve ($\epsilon = 0.016$) was generated by numerical simulation of (3) and (6) using the parameter values in Table 2.

1.2. Leading-Order and Two-Term Approximations of the RC. Mitchell and Schaeffer [20], assuming that the time constants satisfy (7) above, derive the leading-order approximation for the RC associated with the two-current model. Letting $f(\text{DI})$ denote the actual RC obtained numerically from the ODEs (3) and (6), they demonstrate that

$$(11) \quad f(\text{DI}) \sim f_0(\text{DI}) = \tau_{\text{close}} \ln \left[\frac{1 - (1 - h_{\text{min}}) e^{-\frac{\text{DI}}{\tau_{\text{open}}}}}{h_{\text{min}}} \right]$$

as the parameter

$$(12) \quad \epsilon = \frac{\tau_{\text{out}}}{\tau_{\text{close}}}$$

tends to 0. Figure 2(a) shows a comparison of $f_0(\text{DI})$ with actual RCs (obtained numerically) for several choices of ϵ . In each case, $h_{\text{min}} = 1/6$, $\tau_{\text{open}} = 130$ ms, and $\tau_{\text{close}} = 150$ ms. Note that f_0 underestimates the true APD values, although the error does tend to 0 as $\epsilon \searrow 0$.

In the next section, we compute the next-order correction to f_0 . As we shall see,

$$(13) \quad f(\text{DI}) \sim f_0(\text{DI}) + \epsilon^{2/3} f_1(\text{DI}) \quad (\epsilon \searrow 0),$$

where

$$(14) \quad f_1(\text{DI}) = 2.33811 \tau_{\text{close}} \left(\frac{1 - e^{-\frac{\text{DI}}{\tau_{\text{open}}}}}{1 - (1 - h_{\text{min}}) e^{-\frac{\text{DI}}{\tau_{\text{open}}}}} \right).$$

We remark that the DI dependence in (14) is quite weak. Indeed, if $h_{\text{min}} \approx 0$, then the correction term in (13) is approximately equal to the constant $2.33811 \tau_{\text{close}} \epsilon^{2/3}$. Figure 2(b) shows a plot of the leading-order approximation (11), the two-term approximation (13), and the actual RC (obtained numerically) using the parameters in Table 2. Observe that the leading-order approximation considerably underestimates the true APD values, whereas the two-term approximation exhibits excellent quantitative agreement with the actual RC.

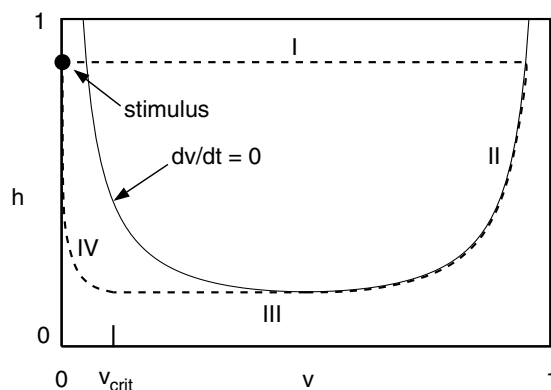


Fig. 3 *Solid curve: the voltage nullcline. Dashed curve: limiting behavior ($\epsilon \searrow 0$) of trajectories in the phase plane for a particular pacing period. The four phases of the action potential are labeled with roman numerals.*

2. Derivation of the Two-Term Asymptotic Approximation. The computations used to derive the two-term asymptotic approximation of $f(\text{DI})$ are similar to those originally performed by Dorodnicyn [7] to estimate the period of the van der Pol oscillator. In preparation for our derivation of (14), we recall the derivation of (11); for details, see Mitchell and Schaeffer [20].

2.1. The Leading-Order Asymptotic Approximation. To leading order, the response of (3), (6) during one pacing period may conveniently be divided into four phases, as labeled in Figure 3:

- Phase I, or upstroke, immediately following a successful stimulus. In a time on the order of τ_{in} , v rises to approximately 1 and h hardly changes.
- Phase II, or plateau. In a time on the order of τ_{close} , h decays from its initial value to h_{min} given by (10), while v follows passively to the value $1/2$. This phase ends when the trajectory “falls off” the nullcline (8).
- Phase III, or repolarization. In a time on the order of τ_{out} , v decays toward 0 while h changes only slightly.
- Phase IV, or DI. For the time remaining until the next stimulus, the gate recovers toward the open state $h = 1$ with a time constant τ_{open} , while v remains close to 0.

The APD consists of all of Phase II and parts of Phases I and III. However, because of (7), to leading order only Phase II contributes to APD. To estimate A_{n+1} , we first examine the recovery of h during the preceding DI. If $t = 0$ corresponds to the beginning of the n th DI, h satisfies the following initial value problem until the $(n + 1)$ th stimulus is applied:

$$(15) \quad \frac{dh}{dt} = \frac{1-h}{\tau_{\text{open}}},$$

$$(16) \quad h(0) = h_{\text{min}}.$$

The value of h at the end of the n th DI is

$$(17) \quad h(D_n) = 1 - (1 - h_{\text{min}})e^{-D_n/\tau_{\text{open}}}.$$

To leading order, h does not change during stimulation or Phase I of the $(n + 1)$ th action potential. Thus A_{n+1} is estimated by the time required for h to decay from $h(D_n)$ to h_{\min} . This yields the approximation

$$(18) \quad A_{n+1} = \tau_{\text{close}} \ln \left[\frac{h(D_n)}{h_{\min}} \right],$$

from which (11) follows.

2.2. The Next-Order Correction. The primary source of error in the leading-order approximation arises from the transition between Phase II and Phase III, which we have called “falling off the nullcline.” Following Mitchell and Schaeffer [20], let us demonstrate that this transition contributes an $O(\epsilon^{2/3})$ correction. Let t^* denote the time in an action potential at which h has decayed to h_{\min} . Then, according to (6),

$$(19) \quad h(t) = h_{\min} e^{-\frac{t-t^*}{\tau_{\text{close}}}}$$

in a neighborhood of $t = t^*$. Inserting (19) into (3), we obtain the nonautonomous equation

$$(20) \quad \frac{dv}{dt} = \frac{v}{\tau_{\text{out}}} \left(\frac{\tau_{\text{out}}}{\tau_{\text{in}}} h_{\min} e^{-\frac{t-t^*}{\tau_{\text{close}}}} v(1-v) - 1 \right),$$

which is valid for t in a neighborhood of t^* . Because $h(t^*) = h_{\min}$, we expect that $v(t^*) \approx \frac{1}{2}$ provided that ϵ is small. Motivated by this observation, we scale time and voltage by introducing “inner” variables

$$(21) \quad \tilde{t} = \frac{t-t^*}{\epsilon^q \tau_{\text{close}}}, \quad \tilde{v} = \frac{v - \frac{1}{2}}{\epsilon^p}.$$

Rewriting (20) in terms of the scaled variables, we have

$$(22) \quad \epsilon^{1+p-q} \frac{d\tilde{v}}{d\tilde{t}} = -\frac{1}{2} \epsilon^q \tilde{t} - 2\epsilon^{2p} \tilde{v}^2,$$

where we have retained only the lowest-order terms. Applying the principle of dominant balance, we require that $1 + p - q = q = 2p$ and hence $p = \frac{1}{3}$ and $q = \frac{2}{3}$. Equation (22) becomes a Riccati equation:

$$(23) \quad \frac{d\tilde{v}}{d\tilde{t}} + 2\tilde{v}^2 + \frac{1}{2}\tilde{t} = 0.$$

Observe that solutions of (23) blow up in finite time for $\tilde{t} > 0$. We use a common trick [11] to convert (23) into a linear equation. Substituting

$$(24) \quad \tilde{v} = \frac{1}{2} \frac{W'}{W}$$

into (23), we find that

$$(25) \quad \frac{1}{2} \left(\frac{W''W - (W')^2}{W^2} \right) + \frac{1}{2} \frac{(W')^2}{W^2} + \frac{1}{2}\tilde{t} = 0.$$

Simplification reveals that W satisfies the Airy equation

$$(26) \quad W'' + \tilde{t}W = 0.$$

The general solution of (26) has the form

$$(27) \quad W(\tilde{t}) = a_0 Ai(-\tilde{t}) + a_1 Bi(-\tilde{t}),$$

where a_0 and a_1 are arbitrary constants² and Ai and Bi are the standard Airy functions. We shall not need their power series representations, which may be found in [11].

From (24) and (27) we find that

$$(28) \quad \tilde{v}(\tilde{t}) = -\frac{1}{2} \cdot \frac{a_0 Ai'(-\tilde{t}) + a_1 Bi'(-\tilde{t})}{a_0 Ai(-\tilde{t}) + a_1 Bi(-\tilde{t})}.$$

To determine the constants a_0 and a_1 , we match to the Phase II outer solution, i.e., let $\tilde{t} \rightarrow -\infty$. The asymptotic behavior of the Airy functions and their derivatives as the argument $x \rightarrow +\infty$ is described by the formulas [11]

$$(29) \quad Ai(x) \sim \frac{1}{2\sqrt{\pi}x^{\frac{1}{4}}} e^{-\zeta}, \quad Ai'(x) \sim \frac{-1}{2\sqrt{\pi}} x^{\frac{1}{4}} e^{-\zeta},$$

$$(30) \quad Bi(x) \sim \frac{1}{\sqrt{\pi}x^{\frac{1}{4}}} e^{\zeta}, \quad Bi'(x) \sim \frac{1}{\sqrt{\pi}} x^{\frac{1}{4}} e^{\zeta},$$

where

$$(31) \quad \zeta = \frac{2}{3}x^{\frac{3}{2}}.$$

Therefore, from (28), (29), and (30) we have

$$(32) \quad \tilde{v} \sim \begin{cases} \frac{1}{2}\sqrt{-\tilde{t}} & \text{if } a_1 = 0, \\ -\frac{1}{2}\sqrt{-\tilde{t}} & \text{if } a_1 \neq 0, \end{cases}$$

as $\tilde{t} \rightarrow -\infty$. In our case, the voltage should increase as $\tilde{t} \rightarrow -\infty$, so we choose $a_1 = 0$. By combining (21) and (28) we obtain the following representation for $v(t)$ with t close to t^* :

$$(33) \quad v(t^* + \epsilon^{\frac{2}{3}}\tau_{\text{close}}\tilde{t}) \sim \frac{1}{2} - \frac{\epsilon^{\frac{1}{3}}}{2} \frac{Ai'(-\tilde{t})}{Ai(-\tilde{t})}.$$

The approximation (33) is valid as \tilde{t} increases until \tilde{t} reaches the first zero of the Airy function $Ai(-\tilde{t})$, which occurs at

$$(34) \quad \tilde{t}_0 = 2.33811\dots,$$

or, in terms of the original time scale, at

$$(35) \quad t = t^* + \tilde{t}_0\tau_{\text{close}}\epsilon^{\frac{2}{3}}.$$

At this time the inner solution (33) blows up, indicating the transition to Phase III, which evolves on a faster time scale. Hence, the time spent falling off the slow manifold lengthens each APD by approximately

$$(36) \quad t_{\text{extra}} \approx \tilde{t}_0\tau_{\text{close}}\epsilon^{\frac{2}{3}}.$$

²Observe that (23) is first order whereas (26) is second order. Upon substituting (27) into (24), we can divide both the numerator and the denominator by a_0 , leaving only one arbitrary constant, a_1/a_0 .

We remark that t_{extra} can be significant relative to the APD values generated by the leading-order estimate of (11). For example, using the parameters in Table 2, we have $\epsilon = 0.016$ and $t_{\text{extra}} > 22$ ms.

This extra time changes A_{n+1} in two ways: directly by adding t_{extra} to (18) and indirectly by modifying the recovery of h during the preceding DI. Specifically, during the extra time added to A_n , h decays³ from h_{\min} to $\exp(-\tilde{t}_0\epsilon^{2/3})h_{\min}$. Therefore, we must replace the initial condition (16) by

$$(37) \quad h(0) = e^{-\tilde{t}_0\epsilon^{2/3}} h_{\min}.$$

This leads to an improved approximation of $h(D_n)$:

$$(38) \quad h(D_n) = 1 - \left[1 - e^{-\tilde{t}_0\epsilon^{2/3}} h_{\min} \right] e^{-\frac{D_n}{\tau_{\text{open}}}}.$$

Making these two adjustments to (18) and expanding in powers of $\epsilon^{2/3}$, we find that $f(\text{DI}) \sim f_0(\text{DI}) + \epsilon^{2/3} f_1(\text{DI})$, where $f_0(\text{DI})$ is given by (11) and

$$(39) \quad f_1(\text{DI}) = \tilde{t}_0 \tau_{\text{close}} \left(\frac{1 - e^{-\frac{\text{DI}}{\tau_{\text{open}}}}}{1 - (1 - h_{\min}) e^{-\frac{\text{DI}}{\tau_{\text{open}}}}} \right).$$

In conclusion, we note that the $O(\epsilon^{2/3})$ -corrections derived above dominate corrections coming from time spent in Phase I or III, since these are $O(\epsilon)$.

REFERENCES

- [1] G. W. BEELER AND H. J. REUTER, *Reconstruction of the action potential of ventricular myocardial fibers*, J. Physiol., 268 (1977), pp. 177–210.
- [2] V. BOOTH, T. W. CARR, AND T. ERNEUX, *Near-threshold bursting is delayed by a slow passage near a limit point*, SIAM J. Appl. Math., 57 (1997), pp. 1406–1420.
- [3] C. M. BENDER AND S. A. ORSZAG, *Advanced Mathematical Methods for Scientists and Engineers*, Springer-Verlag, New York, 1999.
- [4] D. R. CHIALVO, D. C. MICHAELS, AND J. JALIFE, *Supernormal excitability as a mechanism of chaotic dynamics of activation in cardiac Purkinje fibers*, Circ. Res., 66 (1990), pp. 525–545.
- [5] M. COURTEMANCHE, R. J. RAMIREZ, AND S. NATTEL, *Ionic mechanisms underlying human atrial action potential properties: Insights from a mathematical model*, Amer. J. Physiol., 275 (1998), pp. H301–H321.
- [6] E. CYTRYNBAUM AND J. P. KEENER, *Stability conditions for the traveling pulse: Modifying the restitution hypothesis*, Chaos, 12 (2002), pp. 788–799.
- [7] A. A. DORODNICYN, *Asymptotic solution of van der Pol's equation*, Prikladnaya Matematika i Mekanika, 11 (1947), pp. 313–328 (in Russian).
- [8] F. H. FENTON AND A. KARMA, *Vortex dynamics in three-dimensional continuous myocardium with fiber rotation: Filament instability and fibrillation*, Chaos, 8 (1998), pp. 20–47.
- [9] M. R. GUEVARA, G. WARD, A. SHRIER, AND L. GLASS, *Electrical alternans and period doubling bifurcations*, in IEEE Computers in Cardiology, IEEE Computer Society, Silver Springs, MD, 1984, pp. 167–170.
- [10] A. L. HODGKIN AND A. F. HUXLEY, *A quantitative description of membrane current and its application to conduction and excitation in nerve*, J. Physiol. London, 117 (1952), pp. 500–544.
- [11] M. H. HOLMES, *Introduction to Perturbation Methods*, Springer-Verlag, New York, 1995.
- [12] M. S. JAFRI, J. J. RICE, AND R. L. WINSLOW, *Cardiac calcium dynamics: The roles of ryanodine receptor adaptation and sarcoplasmic reticulum load*, Biophys. J., 74 (1998), pp. 1149–1168.

³Recall that h_{\min} represents the smallest h on the nullcline (8), not the smallest h value that can be attained.

- [13] S. S. KALB, H. M. DOBROVOLNY, E. G. TOLKACHEVA, S. F. IDRISSE, W. KRASSOWSKA, AND D. J. GAUTHIER, *The restitution portrait: A new method for investigating rate-dependent restitution*, *J. Cardiovasc. Electrophysiol.*, 15 (2004), pp. 698–709.
- [14] A. KARMA, *Spiral breakup in model equations of action potential propagation in cardiac tissue*, *Phys. Rev. Lett.*, 71 (1993), pp. 1103–1107.
- [15] A. KARMA, *Electrical alternans and spiral wave breakup in cardiac tissue*, *Chaos*, 4 (1994), pp. 461–472.
- [16] J. KEENER AND J. SNEYD, *Mathematical Physiology*, Springer-Verlag, New York, 1998.
- [17] J. KEVORKIAN AND J. COLE, *Perturbation Methods in Applied Mathematics*, Springer-Verlag, New York, 1981.
- [18] C. LUO AND Y. RUDY, *A model of the ventricular cardiac action potential: Depolarization, repolarization and their interaction*, *Circ. Res.*, 68 (1991), pp. 1501–1526.
- [19] C. LUO AND Y. RUDY, *A dynamic model of the cardiac ventricular action potential*, *Circ. Res.*, 74 (1994), pp. 1071–1096.
- [20] C. C. MITCHELL AND D. G. SCHAEFFER, *A two-current model for the dynamics of cardiac membrane*, *Bull. Math. Bio.*, 65 (2003), pp. 767–793.
- [21] D. NOBLE, *A modification of the Hodgkin-Huxley equations applicable to Purkinje fibre action and pace-maker potentials*, *J. Physiol.*, 160 (1962), pp. 317–352.
- [22] J. B. NOLASCO AND R. W. DAHLEN, *A graphic method for the study of alternation in cardiac action potentials*, *J. Appl. Physiol.*, 25 (1968), pp. 191–196.
- [23] A. NYGREN, C. FISET, L. FIREK, J. W. CLARK, D. S. LINDBLAD, R. B. CLARK, AND W. R. GILES, *Mathematical model of an adult human atrial cell: The role of K^+ currents in repolarization*, *Circ. Res.*, 82 (1998), pp. 63–81.
- [24] D. S. ROSENBAUM, L. E. JACKSON, J. M. SMITH, H. GARAN, J. N. RUSKIN, AND R. J. COHEN, *Electrical alternans and vulnerability to ventricular arrhythmias*, *New England J. Med.*, 330 (1994), pp. 235–241.
- [25] D. G. SCHAEFFER, J. W. CAIN, D. J. GAUTHIER, S. S. KALB, W. KRASSOWSKA, R. A. OLIVER, E. G. TOLKACHEVA, AND W. YING, *An ionically based mapping model with memory for cardiac restitution*, *Bull. Math. Biol.*, to appear.
- [26] S. H. STROGATZ, *Nonlinear Dynamics and Chaos*, Addison–Wesley, Reading, MA, 1994.
- [27] M. WATANABE, N. F. OTANI, AND R. F. GILMOUR, JR., *Biphasic restitution of action potential duration and complex dynamics in ventricular myocardium*, *Circ. Res.*, 76 (1995), pp. 915–921.